

## Size-dependent spin-wave frequency in ferromagnetic wire-array structures

A. Ercole, A. O. Adeyeye, J. A. C. Bland, and D. G. Hasko  
*Cavendish Laboratory, Madingley Road, Cambridge CB3 0HE, United Kingdom*  
 (Received 28 October 1997)

Spin-wave frequency measurements in ferromagnetic FeNi wire-array structures by Brillouin light scattering (BLS) are reported. The arrays studied were 600 Å thick and had wire widths of between 0.8 and 10 μm, with separations between wires of twice the width. The spin-wave frequencies were measured in the Voigt geometry with an external field applied parallel or perpendicular to the wires. A rapid drop in BLS intensity with decreasing structure size was seen. For the perpendicular field geometry, we observed a decrease in both the surface and first volume-mode frequencies. We show this to be due to static demagnetizing fields. The parallel field case showed a rise in frequency of only the surface mode with decreasing wire size, which we demonstrate to be the effects of oscillating magnetic edge charges. [S0163-1829(98)04021-1]

### I. INTRODUCTION

Recent advanced lithographic and other controlled preparation techniques have given rise to the possibility of studying magnetism in laterally defined magnetic structures. So far, work has mainly concentrated on the static magnetic properties of such structures.<sup>1-3</sup> Developments in micromagnetic computational techniques<sup>3</sup> have proved important in understanding the observed domain processes.<sup>4</sup> On a fundamental level, the structuring of a thin film into wires gives rise to edge-induced dipolar fields and it is possible to identify shape-induced hard and easy axes for the wires (fields perpendicular and parallel, respectively). This shape anisotropy has a dramatic effect on the static magnetization behavior.

Wire arrays are convenient for magnetoresistance (MR) studies of such effects. A marked size dependence in the easy-axis coercive field and the hard-axis saturation field as the width of the wire is reduced has been seen using transport measurements in submicron structures.<sup>5</sup> A universal behavior of the MR as a function of reduced field normalized to the average demagnetizing field was also found. A transition from bulklike reversal to coherent rotation behavior has been observed in the MR response in noninteracting wire arrays for a field applied perpendicular to the easy axis of the wire as the wire width is reduced from 200 to 2 μm.<sup>1</sup> Coupling between adjacent wires has also been investigated.<sup>6</sup> The details of the field-dependent magnetoresistance were found to be influenced by the separation of the elements. These results were supported by magneto-optical Kerr-effect (MOKE) measurements. Studies of ferromagnetic wires have also been reported by other workers.<sup>7</sup>

The study of magnetic excitations in patterned structures is complicated and has, to date, received little attention. Theoretical work has been confined to the prediction<sup>8</sup> of so-called corner eigenmodes for square magnetic bars. There has been an experimental report of a lateral superlattice effect in coupled grating structures.<sup>9</sup> It has also been suggested that spin waves play a key role in the size scaling of the longitudinal MR response of very fine Ni wires.<sup>10</sup> Further investigation would be of great interest as, if magnetic elements are ever to be used in high-speed electronics, an understanding of their high-frequency response must include an understanding of the spin-wave properties. In this paper, we

report on recent experiments using Brillouin light scattering (BLS) to probe finite-size effects on the spin-wave frequencies in ferromagnetic wire-array structures. We have studied uncoupled wire arrays in order to examine the properties of the individual elements.

The study of spin-wave excitations is a powerful probe of the magnetic properties of laterally defined structures such as the wires considered in this paper. The spin-wave excitations in magnetic materials are described by solutions of the Landau-Lifshitz torque equation:<sup>11</sup>

$$\frac{\partial \mathbf{M}}{\partial t} = \gamma (\mathbf{M} \times \mathbf{H}_{\text{eff}}), \quad (1)$$

where the quantity  $M$  is the magnetic moment of the material and  $\gamma$  is the gyromagnetic ratio which is proportional to the  $g$  factor. The parameter  $H_{\text{eff}}$  (the effective field) is the sum of all magnetic fields present and may have static and time-varying components. Such fields may be of external origin, for example, from some external electromagnet forming part of an experiment. Additionally, there may be contributions from anisotropy and exchange fields. For a general discussion see, for instance, Ref. 12 and the references therein. In laterally defined structures, one must also consider the presence of demagnetizing fields arising from the edges of the elements. Thus it is clear that the dynamic excitations will be directly affected by changes in dimensionality. It would be expected that a study of the spin-wave frequency as a function of in-plane angle would reflect the magnetic symmetry of the wires (a twofold symmetry).

BLS is particularly well suited to the study of magnetic excitations in such structures. First, it is a local probe, the incident light beam being focused onto the sample, allowing small areas to be investigated. Furthermore, BLS allows spin-wave measurements to be made for nonzero in-plane momentum transfer. Typical in-plane wave vectors (IPWV's) probed by BLS are of the order of  $10^5$ – $10^6$  cm<sup>-1</sup> and may be varied by changing the angle of incidence (or the wavelength of the light source). This allows in-plane dipolar effects associated with nonuniform magnetization distributions to be studied. If the spin-wave IPWV is perpendicular to the wire, we also expect finite-size effects associated with spin-wave confinement to become apparent when the wire size becomes comparable to the spin-wave wavelength being

probed. The separation between the wires defines an additional length scale for interwire dipolar coupling. In the work presented in this paper, we have attempted to minimize this coupling by fabricating samples with a separation between wires of twice the wire width. From MR measurements,<sup>1</sup> we infer that the wires in such arrays are indeed uncoupled.

Just as in the static investigations, it is possible to measure hard- and easy-axis responses using BLS. We consider only the case where the spin-wave frequencies probed are for excitations with their IPWV's perpendicular to the applied field (as is the case for measurements in the Voigt scattering geometry used here). For the hard-axis case, where the spins are forced by an external field into saturation perpendicular to the wires, a static demagnetizing field is to be expected. This arises from magnetic charges at the edges and is subtractive from the applied field. For a given magnetization, this demagnetizing field will be expected to increase as the wire width is decreased. Thus, we expect that the parameter  $H_{\text{eff}}$  in Eq. (1) will be reduced as the wires are made narrower. The restoring torque on the individual spins is therefore also reduced and the spin-wave frequency will drop as the wire width is reduced.

Let us now consider the easy-axis case when the applied field is arranged to orient the magnetization along the wires. For this magnetic configuration, there are no static magnetic poles present on the wire edges as there is no component of the magnetization perpendicular to the wires, and so there is no static demagnetizing field as in the hard-axis case. However, in a spin-wave excitation, the spins precess about the equilibrium position. This gives rise to a small, time-varying, magnetization perpendicular to the edges (and the top and bottom surfaces) of the wires. Thus, the spin-wave itself can supply a time-varying polarization that can generate a dynamic demagnetizing field which could, in turn, influence the spin-wave frequency. In the long-wavelength limit, where the excitations on both sides of the wire are in phase, this dynamic field always serves as a restoring torque and so the spin-wave frequency can be expected to increase as the wire width is decreased. This can be thought of as a confinement effect as the presence of the wire edges tends to reduce the spin-precession amplitude.

Let us consider this behavior more quantitatively. Within a simple model considering isolated spins, we may construct solutions to Eq. (1). We shall neglect any exchange contribution to the surface-mode frequencies, as this will be small for such small angles of incidence (small IPWV). Intrinsic anisotropy contributions will also be assumed to be small. This will be shown to be a good approximation for the structures investigated here. We shall also assume that the spin waves are not pinned at the edges of the wires. Such pinning would alter the boundary conditions to reduce the precession amplitude at the wire edges, and so the dynamic demagnetizing fields would be diminished. As before, we neglect the spatial variations in the demagnetizing field that must be present for nonellipsoidal bodies. Except near the edges of the structures, such variations are relatively small compared with the magnitude of the demagnetizing field at the center of the wire. The trial solutions must contain additional field terms that reflect the oscillating demagnetizing fields due to the components of the dynamic magnetization at the wire edges and the top and bottom surfaces;

$$\mathbf{M} = M_0 \mathbf{i}_z + \mathbf{m} e^{-j\omega t},$$

$$\mathbf{H} = H_0 \mathbf{i}_z - N_x m_x e^{-j\omega t} \mathbf{i}_x - (1 - N_x) m_y e^{-j\omega t} \mathbf{i}_y, \quad (2)$$

where we have taken the applied field  $H_0$  to be along the  $z$  axis. The  $x$  axis is across the width of the wire and the  $y$  axis is therefore along the length of the wire.  $M_0$  is the static magnetization and components of  $\mathbf{m}$  and  $\mathbf{h}$  represent the dynamic (spin-wave) magnetization which are assumed to be small in comparison to  $M_0$ .  $N_x$  is the demagnetizing factor. We have made use of the relation

$$1 = N_x + N_y + N_z \quad (3)$$

and that  $N_z \approx 0$  since these wires are long. By substituting into the Landau-Lifshitz equation, and linearizing, we obtain an expression for the frequency:

$$\left(\frac{\omega}{\gamma}\right)^2 = (H_0 + 4\pi M N_x)[H_0 + 4\pi M(1 - N_x)]. \quad (4)$$

The above expression is derived for a collection of isolated spins. It would be expected to hold for spin waves in the long-wavelength limit, where all spins are precessing in phase. However, the precise nature of the dynamic demagnetizing fields will depend on the details of the mode profile and is expected to be different for volume modes, for example.

Let us qualitatively consider the hard-axis behavior for surface spin waves of shorter wavelength (larger IPWV). In the limit of very short wavelength, nearby spins will be out of phase. Since this will also be true near the wire edges, the amplitude of the oscillating magnetizing at the edges (and so also the dynamic demagnetizing field) will be reduced. Thus, the confinement effect described above is predicted to vanish. This is to be expected as, in the short-wavelength limit, the wires appear effectively infinite, even for excitations traveling across their width. For intermediate-wavelength spin waves, the details of the dynamic demagnetizing field amplitude distributions will be strongly wavelength dependent.

## II. EXPERIMENT

Our samples consisted of 600 Å thick Fe<sub>20</sub>Ni<sub>80</sub> wire arrays in the 0.8–10 μm size width range and were prepared from continuous films grown by ultrahigh-vacuum electron-beam evaporation onto GaAs(001) substrates. This material is particularly suitable as it is magnetically isotropic, and also has a very narrow natural spin-wave linewidth which is useful for accurate measurements. The vacuum system has a base pressure of  $5 \times 10^{-10}$  mbar. The substrates were held at 30 °C and the growth rate was 2.5 Å/min. The films were annealed at 120 °C for 30 min to remove the uniaxial anisotropy induced during growth. The wire arrays were fabricated (see Fig. 1) using electron-beam lithography and optimized pattern transfer techniques based on a combination of dry and wet etching. The details of the fabrication process have been described elsewhere.<sup>13</sup> All wire arrays for which data are presented here were prepared in 0.3×0.3-mm patches on the same FeNi film, thus ensuring that the material parameters were the same for all samples. MOKE measurements

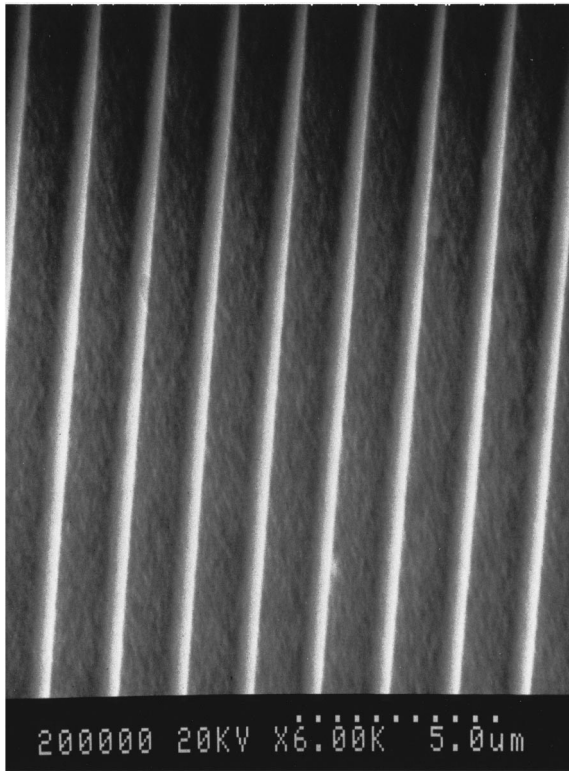


FIG. 1. Scanning electron micrograph of typical wire-array structure demonstrating the good edge acuity achieved. This sample had been deep-etched into the GaAs substrate to provide contrast for microscopy.

on an unpatterned control patch before and after processing showed no noticeable sample degradation by the processing technique. This indicates that our patterning technique causes minimal sample damage. It is worth noting, however, that in samples prepared by dry etching alone, a dramatic broadening of the spin-wave line shape was observed, which is believed to be due to sample damage. It was not possible to obtain useful BLS measurements from such samples. All our samples were fabricated with wire separations of twice the wire width.

The main elements of our BLS apparatus have been described previously.<sup>14</sup> Additionally, the original stabilization system has been replaced by a computer-controlled system.<sup>15</sup> This afforded the experiment with superior long-term stability compared to the original analog-based stabilization. This was found to be essential as the spin-wave signals from the smallest wires studied were of very low intensity making long spectrum acquisition times necessary. A single-mode argon-ion laser was used to provide 100 mW of 514.5-nm wavelength light which was focused onto the sample. The backscattered radiation was collected and frequency analyzed by a 3+3 pass tandem Fabry-Pérot interferometer. The scattering plane was at right angles to the field (Voigt geometry). The incident beam was accurately positioned onto the wire arrays by monitoring the back-reflected diffraction pattern. Careful masking of these diffracted beams was required to prevent them from entering and blinding the interferometer.

The sample was mounted on an  $xyz$  manipulator, itself mounted on a rotation stage. This stage was, in turn attached

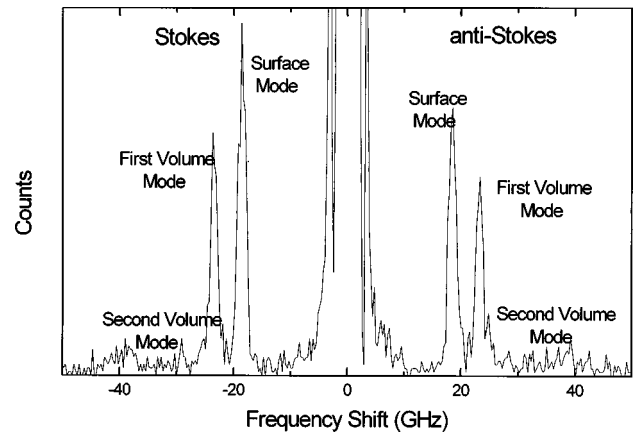


FIG. 2. BLS spectrum of the unpatterned FeNi film. The large central feature is the inelastic Rayleigh peak. At least three modes are visible in both the Stokes and anti-Stokes regions of the spectrum.

to a single-axis goniometer, which could rotate about the external (applied) field axis. With this system it was therefore possible to arrange for any patch to be brought into focus accurately at the center of the magnet pole pieces, with the light incident at any angle from  $0^\circ$  to nearly  $90^\circ$  (to change the spin-wave IPWV being probed) and with the wires at any angle to the in-plane applied field. As the magnet was capable of fields up to 10 kOe, and precise alignment was of importance, the sample manipulator was designed to be substantially free of magnetic components.

### III. RESULTS AND DISCUSSION

A typical BLS spectrum from the unpatterned patch is shown in Fig. 2. At least three spin-wave modes can be seen. The modes were found to have narrow linewidths, as is typical of FeNi. They may be classified as follows. The spin-wave mode solutions to the Landau-Lifshitz equation in films of this thickness may be either of Damon-Eshbach surface or volume type.<sup>16-19</sup> The surface modes exhibit an exponential decay of the dynamic magnetization amplitude away from the surface. There exist two frequency-degenerate and counterpropagating modes; one for each surface. The Stokes and anti-Stokes surface-mode peaks (corresponding to spin-wave creation and annihilation events, respectively) generally have different intensity due to the nonreciprocal propagation of this type of mode.<sup>17,19</sup> Volume modes, which have standing-wave-type behavior due to confinement perpendicular to the film plane are also observed in films greater than about 150 Å thick. The first volume mode has one node and is an antisymmetric function of depth across the film. The higher-order volume modes have successively more nodes. Measurements of the spin-wave frequencies as a function of in-plane angle for the unpatterned film are shown in Fig. 3. To within errors, these were constant, demonstrating that any residual intrinsic anisotropy was less than about 5 Oe. In combination with measurements of frequency as a function of applied-field strength, it is possible to extract values for  $M=800$  Oe,  $g=2.09$  required for the interpretation of the results for the wires. Such an analysis was based on the formulation of Hicken *et al.*<sup>20</sup>

It was not possible to observe modes other than the sur-

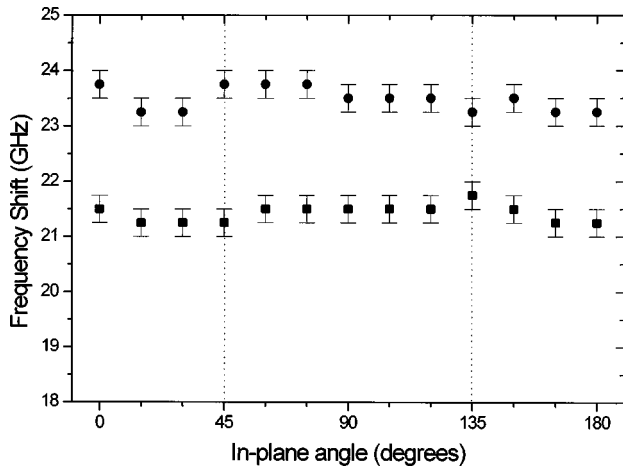


FIG. 3. Spin-wave frequencies as a function of in-plane applied field angle for the unpatterned patch. The angle of incidence was  $45^\circ$  and the applied field was 3 kOe in magnitude.

face and first volume modes in the wire arrays. The inelastic signal intensity was observed to drop rapidly with reducing wire size raising spectrum acquisition times from 20 min to up to 7 h in the smallest wires measured. This is, perhaps, surprising as the wires are always separated by twice the width. Thus the same quantity of magnetic material is always present. The mode line shapes and linewidths were carefully studied at various angles of incidence. We found no evidence of any mode splitting associated with possible zone folding due to the lateral periodicity of these structures from the line shape. The linewidths were also found to be independent of the wire width. These observations suggest that the spin-wave excitations are not coherent between wires. As the wire width is reduced, and the total magnetic material present becomes more finely divided, the scattering becomes increasingly incoherent, and the intensity is reduced. This is consistent with adjacent wires being uncoupled.

Figure 4 shows a similar angle scan, but now for the case

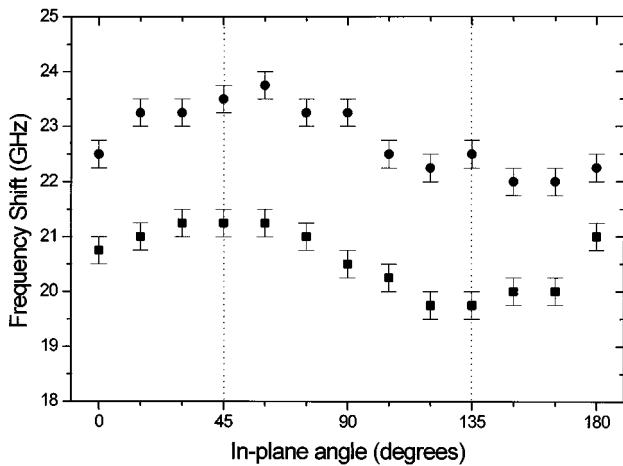


FIG. 4. Spin-wave frequencies as a function of in-plane applied field angle for the  $1 \mu\text{m}$  wide wire-array patch. The angle of incidence was  $45^\circ$  and the field was 3 kOe in magnitude. The direction marked as  $45^\circ$  corresponds to the wires being oriented along the applied field (i.e.,  $135^\circ$  represents the perpendicular configuration). The twofold symmetry is clearly discernible.

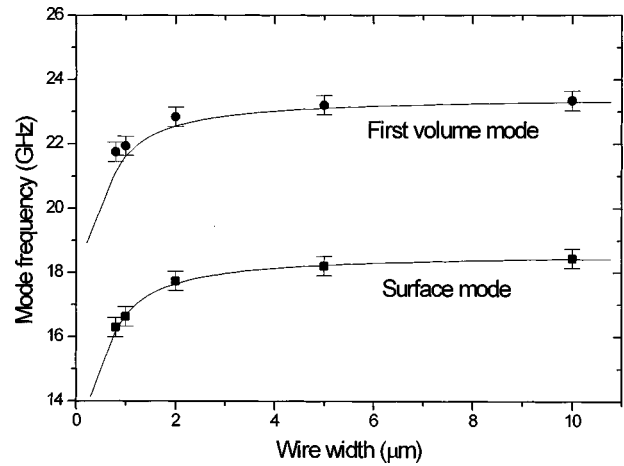


FIG. 5. Spin-wave frequencies as a function of wire width in the perpendicular field configuration. The field was 3 kOe in magnitude and the angle of incidence was  $5^\circ$ . The solid lines represent the static demagnetizing field predictions as described in the text.

of the array of  $1 \mu\text{m}$  wide wires. A very clear twofold (uniaxial) anisotropy is seen to have been introduced. This is as expected from consideration of the new in-plane symmetry and arises from the presence of demagnetizing fields from the wire edges as described above. Such angle scans are laborious to obtain with high precision at each point. To examine the size dependencies further, we have performed more accurate measurements at the principle directions, i.e., with the wires parallel (easy axis) and perpendicular (hard axis) to the field.

A summary of the results for the case of the applied field being perpendicular to the wires is presented in Fig. 5, where the frequencies of the surface and first volume mode are shown as functions of wire width. Both modes were observed to show a drop in frequency with reducing wire width. We attribute this effect to the presence of static demagnetizing fields arising from magnetic charges at the edges of the wires, which have been measured in static magnetometry and MR experiments<sup>1</sup> as described in the Introduction. To test this simple interpretation, we have per-

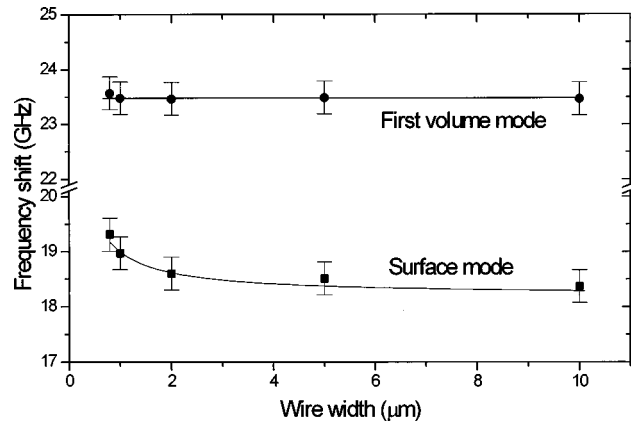


FIG. 6. Spin-wave frequencies as a function of wire width in the parallel field configuration. The field was 3 kOe in magnitude and the angle of incidence was  $5^\circ$ . The solid line through the surface mode points is a plot of Eq. (4), using the material parameters derived from a fit to the data presented in Fig. 3.

formed spin-wave frequency calculations using the method given in Ref. 20, but taking the additional demagnetizing field into account. The calculation involves the solution of Eq. (1) and the Maxwell equations with the general Rado-Weertman exchange-boundary condition.<sup>21</sup> This method, which proceeds numerically, is necessary to model the volume modes and accurately predict the mode frequencies in films of this thickness. The demagnetizing field for square section wires can be calculated numerically according to the prescription given in Ref. 21. We have used the first-order approximation of uniform magnetization within the wire. As the elements are not ellipsoidal, the calculated field is a function of position within the wire.<sup>22</sup> However, for the spin-wave calculations, we neglect this variation (which is not large, except near the wire edges) and use the value for the center of the wire. Such approximations have been shown to be valid in the modeling of MR data.<sup>1</sup> The results of such calculations are shown as the curves in Fig. 3. A good agreement between the model and the experimental results is apparent. This interpretation is also in good agreement with MOKE magnetometry data which revealed a reversible hard-axis behavior with a saturation field which increased with decreasing wire width due to the increasing demagnetizing field.

Figure 6 shows the analogous data, but for the case of the applied field being parallel to the wires (i.e., the scattering vector is perpendicular to the wires). For this configuration the frequency of the surface mode was seen to be increased, as predicted, in the samples with smaller wire width. The volume-mode frequency appears to be substantially unaffected by the wire width in this geometry. The expression given in Eq. (4), using the material parameters already determined, and the calculated demagnetizing factors, is plotted as the solid curve through the surface-mode points in Fig. 6. It can be seen that the agreement is good. This indicates that the spins experience the full dynamic demagnetizing field, which implies that there is little pinning of the spin waves at the wire edges.

A study of the parallel field behavior with scattering angle showed that the confinement effect disappeared for angles away from normal incidence. This is in accordance with the reduction in the confinement effect at larger IPWV predicted above. No particularly remarkable behavior was identified at ‘‘Bragg’’ or ‘‘anti-Bragg’’ conditions [ $n\lambda = 2w \sin \theta$  and  $(n + \frac{1}{2})\lambda = 2w \sin \theta$ , respectively, for an angle of incidence of  $\theta$ ], but this is not surprising as even the frequency shifts observed near normal incidence were near the limit of our resolution.

A model which predicted the first volume mode behavior would have to include the exchange interaction. However, since the mode amplitude profile has a change of sign with

depth, the dynamic demagnetizing fields will substantially cancel and, to a first approximation, the frequency would be expected to thus be insensitive to wire width as is indeed observed.

#### IV. SUMMARY AND CONCLUSIONS

In summary, we have measured spin-wave frequencies in arrays of uncoupled ferromagnetic wires with widths in the range 0.8–10  $\mu\text{m}$ . We have shown how these frequencies are affected by the finite width of the wires. This effect is of different origin for the perpendicular and parallel field cases described. These have been shown to be static and dynamic effects, respectively. Both effects, however, are mediated by the same geometrical demagnetizing factor. In both cases, we have observed a drop in inelastic intensity, which we attribute to the crossover from a coherent scattering regime, to an increasingly incoherent scattering regime as the wire widths were reduced, and the magnetic film becomes increasingly disconnected.

In the parallel case, our results indicate that the effect of the confinement depends on the details of the dynamic magnetization profiles within the film, as we observe that the surface and first volume modes are differently affected by the reduced wire width. We have shown how the surface-mode behavior can be accounted for within a simple model, and how this model is consistent with the volume-mode behavior. As the confinement frequency shifts were so small, we were unable to make a detailed study as a function of IPWV. It would be of interest to investigate the spin-wave frequencies at successive ‘‘Bragg’’ and ‘‘anti-Bragg’’ conditions. Such experiments would be facilitated if spin waves could be measured in high-quality wire arrays, 0.1  $\mu\text{m}$  in width or less, in which the demagnetizing fields would be expected to be much larger.

It is hoped that this work will stimulate further theoretical interest in modeling spin-wave modes not only in wires, but also in other structures, both in the uncoupled and coupled cases. Such a description of the response of wires to the complicated dynamical field distributions that can occur will be necessary to understand the spin-wave behavior in the next generation of lithographically produced magnetic structures.

#### ACKNOWLEDGMENTS

The authors gratefully acknowledge the financial support of the EPSRC and the EC-ESPRIT programme in this project and thank Dr. R. J. Hicken and Dr. B. E. Camley for useful discussions and suggestions. We would also like to thank Professor H. Ahmed for assistance with sample structuring.

<sup>1</sup>A. O. Adeyeye, J. A. C. Bland, C. Daboo, J. Lee, U. Ebels, and H. Ahmed, *J. Appl. Phys.* **79**, 6120 (1996).

<sup>2</sup>C. Shearwood, S. J. Blundell, M. J. Baird, J. A. C. Bland, M. Gester, H. Ahmed, and H. P. Hughes, *J. Appl. Phys.* **75**, 5249 (1994).

<sup>3</sup>J. F. Smyth, S. Schultz, D. R. Fredkin, D. P. Kern, S. A. Rishton,

H. Schmid, M. Cali, and T. R. Koehler, *J. Appl. Phys.* **69**, 5262 (1991).

<sup>4</sup>E. Gu, E. Ahmad, S. J. Gray, C. Daboo, J. A. C. Bland, L. M. Brown, M. Rühlig, A. J. McGibbon, and J. N. Chapman, *Phys. Rev. Lett.* **78**, 1158 (1997).

<sup>5</sup>M. H. Kryder, K. Y. Ahn, N. J. Mazzeo, S. Schwarzl, S. M. Kane,

- IEEE Trans. Magn. **MAG-16**, 99 (1980).
- <sup>6</sup>A. O. Adeyeye, J. A. C. Bland, C. Daboo, and D. Hasko, Phys. Rev. B **56**, 3265 (1997).
- <sup>7</sup>Y. Otani, B. Pannetier, J. P. Nozieres, and D. Givord, J. Magn. Mater. **126**, 622 (1993).
- <sup>8</sup>T. M. Sharon and A. A. Maradudin, J. Phys. Chem. Solids **38**, 971 (1977).
- <sup>9</sup>B. A. Gurney, P. Baumgart, V. Speriosu, R. Fontana, A. Patlac, T. Logan, and P. Humbert (unpublished).
- <sup>10</sup>K. Hong and N. Giordano, Phys. Rev. B **51**, 9855 (1995).
- <sup>11</sup>L. D. Landau and E. M. Lifshitz, Phys. Z. Sowjetunion **8**, 153 (1935).
- <sup>12</sup>B. Heinrich and J. F. Cochran, Adv. Phys. **42**, 523 (1993).
- <sup>13</sup>A. O. Adeyeye, J. A. C. Bland, C. Daboo, D. G. Hasko, and H. Ahmed, J. Appl. Phys. **82**, 469 (1997).
- <sup>14</sup>R. J. Hicken, A. J. R. Ives, D. E. P. Eley, C. Daboo, J. A. C. Bland, J. R. Childress, and A. Schuhl, Phys. Rev. B **44**, 9348 (1991).
- <sup>15</sup>The computer-controlled spectrum acquisition and stabilization system was developed by B. Hillebrands and co-workers. (Present address: Fachbereich Physik, Universität Kaiserslautern, Germany.)
- <sup>16</sup>R. W. Damon and J. R. Eshbach, J. Phys. Chem. Solids **19**, 308 (1961).
- <sup>17</sup>G. Rupp, W. Wettling, R. S. Smith, and W. Jantz, J. Magn. Mater. **45**, 404 (1984).
- <sup>18</sup>R. E. Camley, T. L. Rahman, and D. L. Mills, Phys. Rev. B **23**, 1226 (1981).
- <sup>19</sup>C. E. Patton, Phys. Rep. **103**, 251 (1984).
- <sup>20</sup>R. J. Hicken, D. E. P. Eley, M. Gester, C. Daboo, A. J. R. Ives, and J. A. C. Bland, J. Magn. Mater. **145**, 278 (1995).
- <sup>21</sup>G. T. Rado and J. R. Weertman, J. Phys. Chem. Solids **11**, 315 (1959).
- <sup>22</sup>R. I. Joseph and E. Schloemann, J. Appl. Phys. **36**, 1579 (1965).